PACS numbers: 52.80Yr; 42.72.Bj
DOI: 10.1070/QE2005v035n07ABEH008967

High-power spontaneous UV radiation source and its excitation regimes

E.Kh. Baksht, M.I. Lomaev, A.N. Panchenko, D.V. Rybka,
V.F. Tarasenko, M. Krishnan, J. Thompson

Abstract. **Different excitation regimes of a discharge in a xenon flashlamp are studied. It is shown that in passing from the oscillating discharge current to the unidirectional current pulse, the UV power radiation increases, while the FWHM of the radiation pulses decreases. The maximum UV power density of the discharge restricted by the flashlamp tube walls was ~ 700 and ~ 380 kW cm^{-2} on the internal and external surfaces of the flashlamp tube, respectively.**

Keywords: *pulsed Xe flashlamp, UV radiation source, excitation regime, gas-discharge excitation regime.*

1. Introduction

Over more than the last two decades the attempts have been made to develop an efficient radiation source to control a high-voltage diamond switch [1 – 3]. The control of this switch by an electron beam [4] and a UV laser [5] has been demonstrated. However, an electron accelerator and a laser are too complicated and expensive to be used in industrial switches. In this connection it is necessary to create a high-power and moderately priced UV radiation source to control the diamond switch [6, 7]. This source should emit microsecond pulses predominantly in the UV region (the fundamental absorption band of a diamond crystal lies in the wavelength range $\lambda \leqslant 225$ nm, while impurities absorb at $\lambda > 225$ nm [8, 9]). Noble gas-discharge flashlamps are promising radiation sources for this spectral region [10]. These lamps are used, for example, for UV pumping organic dye lasers. Compared to discharges in other noble gases, a discharge in xenon has the largest gradient of the potential and the smallest voltage drop in near-electrode regions, so that it is most efficient for using in flashlamps [11].

The aim of this paper is to find the Xe discharge regimes providing an increase in the power and power density of microsecond radiation pulses in the spectral range between 200 and 400 nm.

E.Kh. Baksht, M.I. Lomaev, A.N. Panchenko, D.V. Rybka, V.F. Tarasenko Institute of High Current Electronics, Siberian Branch, Russian Academy of Sciences, prosp. Akademicheskii 2/3, 634055 Tomsk, Russia; e-mail: VFT@loi.hcei.tsc.ru;
M. Krishnan, J. Thompson Alameda Applied Sciences Corporation, 94577 San Leandro, CA, USA

Received 18 April 2005
Kvantovaya Elektronika **35** (7) 605 – 610 (2005)
Translated by M.N. Sapozhnikov

2. Experimental

The discharge in xenon was produced by using a pulsed generator, whose electric circuit is presented in Fig. 1. Such a generator was earlier employed for pumping different lasers and is described in detail in [12]. Three operating regimes of the generator were used in experiments. In regime 1, the generator operated with switched off SOS (semiconductor opening switch) diodes (a conventional electric circuit of the LC generator consisting of a storage capacitor C_0, a trigatron switch K_0, the inductance of the discharge circuit connections and a flashlamp placed in series). Regime 2 differed from regime 1 by the connection of SOS diodes in parallel with the flashlamp (up to 24 SOS diodes were connected). In regime 3, the discharge current of an additional capacitor C_1 was preliminary passed through the SOS diodes in the forward direction (the block of direct pumping of SOS diodes is outlined by the dashed line in Fig. 1) and then, after switching on the switch K_0, in the backward direction, which resulted in the current breaking in SOS diodes and formation of a high-voltage pulse [13]. This was accompanied by the breakdown of the discharge gap in the flashlamp and switching of the current flowing through SOS diodes to the discharge gap.

The capacitances of capacitors used in experiments were $C_0 = 260 - 376$ nF, $C_1 = 34 - 110$ nF and their charging voltages were $U_0 = 0 - 30$ kV and $U_1 = 0 - 35$ kV. The SOS diodes with the reverse voltage up to 50 kV and breaking current up to 2 kA were used in the generator.

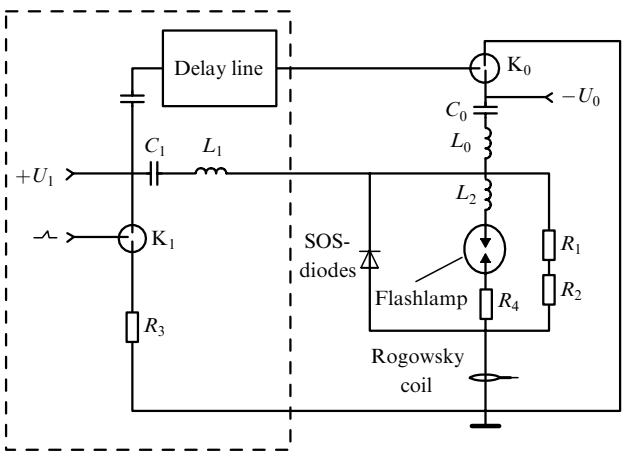

Figure 1. Electrical circuit of the experimental setup.

The parameters of a freely expanding discharge and a discharge restricted by the flashlamp tube walls were compared by exciting the flashlamp using an *LC* generator with a storage capacitor of 165, 266, 376 or 1376 nF and the charging voltage up to 35 kV.

The flashlamp was filled with xenon at a pressure of 50 – 1000 Torr. The interelectrode gap was varied from 2 to 23 mm. The cylindrical flashlamp tube with an internal diameter of 20 mm was made of quartz transmitting no less than 85 % of radiation in the spectral region from 200 to 400 nm. In experiments with a discharge restricted by the flashlamp walls, a similar flashlamp tube of internal diameter 3 mm was used.

The optical characteristics were recorded with an EPP2000C-25 spectrometer equipped with a CCD linear array (sensitive in the 220 – 850-nm spectral range) and a FEK-22SPU coaxial photocell (sensitive in the 200 – 650-nm range). The discharge emission was photographed with a SensiCam CCD camera [7]. Discharge current and voltage pulses on the flashlamp electrodes were detected with a current shunt R_4, a Rogowsky coil, and an ohmic voltage divider R_1, R_2, whose output signals were fed into a Tektronix TDS-224 oscilloscope.

3. Experimental results and discussion

We studied different regimes of the energy input to the discharge, as well as regimes of the freely expanding discharge and the discharge restricted by the quartz tube walls.

The interelectrode gap and Xe pressure in the flashlamp were preliminary optimised. Figure 2 shows the dependences of the peak radiant intensity and linear peak radiant intensity on the interelectrode gap. In this case, the Xe pressure was 400 – 600 Torr (depending on the interelectrode gap) and was selected to obtain the maximum UV radiation intensity for a given interelectrode gap. Our experiments showed that, as the interelectrode gap decreased from 4 to 2 mm, the relative intensity of UV radiation in the emission spectrum increased, but the peak radiant intensity drastically decreased (Fig. 2). When the interelectrode gap exceeded 4 mm, the intensity of the emission spectrum below 250 nm, where a diamond crystal absorbs light most efficiently, decreased, i.e., the spectral efficiency in this wavelength region decreases (Fig. 3). The optimal interelectrode gap in all the successive experiments was 4 mm.

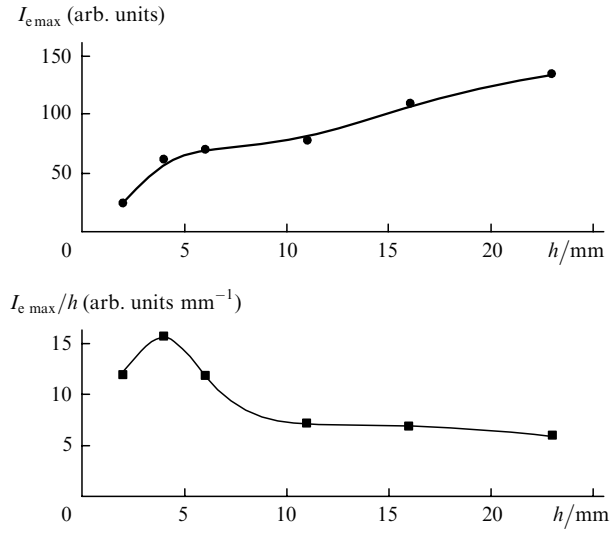

Figure 2. Dependences of the peak radiant intensity $I_{e\,max}$ and linear peak radiant intensity $I_{e\,max}/h$ of a Xe flash lamp in the wavelength range 200 – 850 nm on the interelectrode gap h in regime 1 for $C_0 = 233$ nF and $U_0 = 15$ kV.

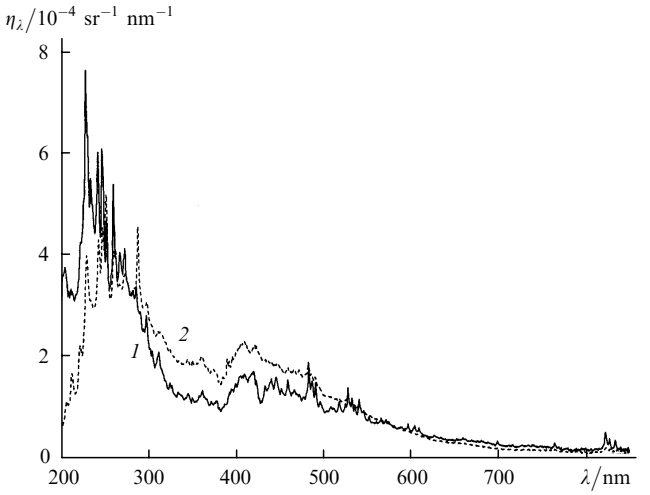

Figure 3. Spectral efficiency η_λ of the Xe flashlamp with the interelectrode gap $h = 4$ (*1*) and 23 mm (*2*).

The operating Xe pressure in the flashlamp was selected based on the following considerations: a pressure is changed from 50 to 100 – 300 Torr, the peak radiation power of the discharge increases, while at $p > 300$ Torr, this increase almost ceases, although the energy input to the discharge and the radiation energy continue to increase. At the same time, at pressures of the order of atmospheric and greater energy inputs, a quartz flashlamp tube was destructed. Therefore, we selected the operating pressure $p = 550$ Torr, which allowed us to work at rather high radiation energies and to obtain high peak powers.

By studying the regimes of energy input to the discharge, we recorded the discharge current, voltage across electrodes, power and emission spectrum of the discharge, and photographed the discharge emission at different instants with a CCD camera. Figure 4 shows the current oscillograms and time dependences of the radiant intensity in the Xe discharge at different voltages for regimes 1 and 3 of the generator operation. Curves (*1*) and (*2*) in Fig. 4 correspond to the oscillating current regime in the discharge, while curves (*3*) and (*4*) correspond to the unidirectional current pulse regime.

One can see that in the case of a unidirectional discharge current pulse, the radiation power and the radiant intensity of the flashlamp, proportional to the radiation power, increase, whereas the FWHM of the radiation pulse decreases. Even a greater increase in the radiation power was achieved in regime 2 of the pulsed generator because in this regime there are no losses in SOS diodes at the direct pumping and current breaking stages.

Unlike regime 1 (*LC* generator), in regimes 2 and 3 during the discharge of the capacitor C_0 when the voltage polarity across SOS diodes was changed from reverse to forward, the diodes shunted the inductance L_2 through the

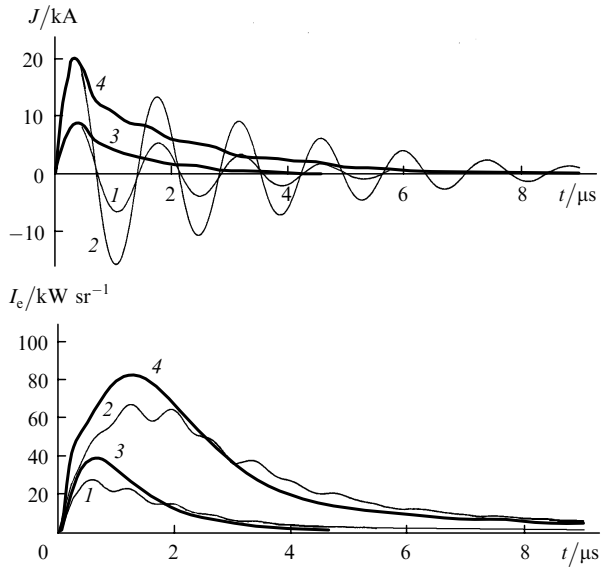

Figure 4. Discharge current J and the radiant intensity I_e of the Xe flashlamp in the wavelength range 200–850 nm in regimes 1 [(*1*), (*2*)] and 3 [(*3*), (*4*)] for $C_1 = 34$ nF, $U_1 = 15$ kV [(*3*), (*4*)], $U_0 = 9.5$ [(*1*), (*3*)] and 24 kV [(*2*), (*4*)], $C_0 = 260$ nF, and $L_2 = 170$ nH.

lamp. Note that at the instant of changing of the voltage polarity across diodes, the current achieved the value close to maximal because the active resistance of the switch K_0–storage capacitor C_0–flashlamp circuit was already much lower than its wave resistance. The inductance L_2 began to release the energy stored by this time over a newly formed L_2–SOS diodes–flashlamp circuit. The discharge current of inductance L_2 in this circuit decreased exponentially, with the time constant $\tau \sim L_2/R_a$, where R_a is the active resistance of the circuit. At the same time, the discharge current of the capacitor C_0 flowing through the SOS diodes–flashlamp circuit, measured with a Rogowsky coil (Fig. 1), represented damped oscillations.

The increase in the peak radiation power of the flashlamp in regimes 2 and 3 compared to regime 1 can be explained by the absence of oscillations of the electric power released in the discharge (excitation power). Upon excitation of the flashlamp by the generator in regime 1 (*LC* generator), the discharge current oscillates, which results in inevitable pulsations of the excitation power. As this power is decreased to zero, the discharge plasma is efficiently cooled. This in turn causes pulsations of the radiation power [curves (*1*) and (*2*) in Fig. 4]. As the voltage U_0 increases, the redistribution of the power in the peaks of the excitation pulse occurs (the peak corresponding to the second half-period of the current increases). In regimes 2 and 3, the current flows through the flashlamp in one direction and, unlike regime 1, the power supplied to the discharge almost does not exhibit pulsations. This leads to an increase in the peak power and a decrease in the FWHM of the radiation pulse compared to those in regime 1.

Regime 2 differs from regime 3 by the absence of a short high-voltage pulse, which is formed upon current breaking in SOS diodes and ignites a discharge in the flashlamp at high pressures and a large interelectrode gap. Note that the charging voltage of the capacitor C_0 was sufficient for a stable breakdown of xenon in the flashlamp in regime 2. In regime 3, the additional possibility appears to change the current J_{sw} switched from SOS diodes to the flashlamp (Fig. 5) by varying the breaking current. An increase in the switched current provides an increase in the power released in the discharge at the initial stage.

Figure 5 shows the typical oscillogram of the current flowing through the flashlamp in regime 3. The attempts to reduce the ratio J_{max}/J_{sw} (Fig. 5) resulted in this case in a decrease in the peak radiant intensity of the flashlamp compared to that in regime 2. This is clearly demonstrated in Fig. 6, where the experimental dependences of the peak radiant intensity $I_{e\,max}$ of the flashlamp in the 200–850-nm range on the energy W_0 stored in the generator are presented. The points corresponding to the generator operation in regime 2 are well fitted by the straight line $I_{e\,max} \sim W_0^{0.5} = (C_0 U_0^2/2)^{0.5}$ (dashed straight line in Fig. 6). A similar empirical dependence is valid for the peak radiant intensity [14]. The ratio J_{max}/J_{sw} was reduced from 1.92 to 1.1 by decreasing the voltage U_0 from 30 kV to zero (the voltage U_1 remained equal to 35 kV). As U_0 was increased, the ratio J_{max}/J_{sw} increased, the relative energy losses in SOS diodes decreased [13] (with respect to the energy stored in the generator) and the peak radiation powers of the flashlamp in regimes 3 and 2 became equal for the same stored energy.

For $U_0 = 30$ kV (regime 2), the radiation energy in the 200–400-nm range achieved ~ 2 J. Note that the peak radiation power in regimes 2 and 3 increases compared to that in regime 1 at approximately the same energies of the radiation pulse.

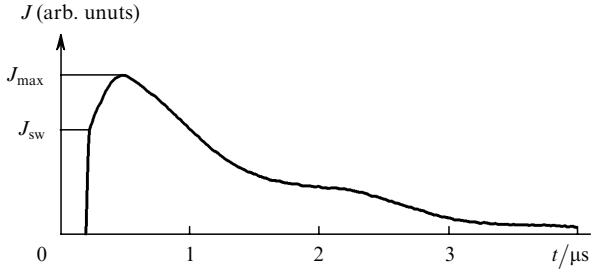

Figure 5. Oscillogram of the current J through the flashlamp in generator regime 3.

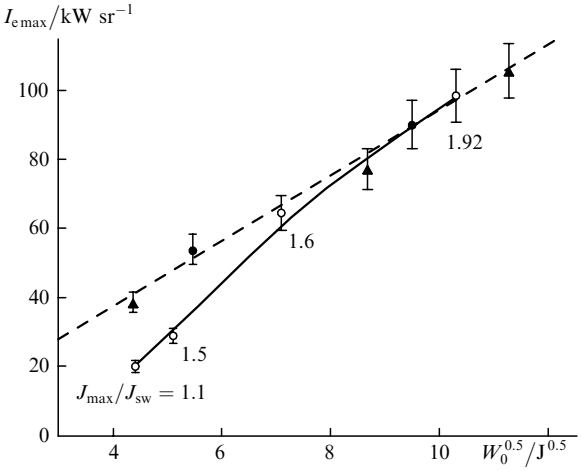

Figure 6. Dependences of the peak radiant intensity $I_{e\,max}$ of the flashlamp in the wavelength range 200–850 nm on $W_0^{0.5}$ in regime 3 for $C_0 = 266$ nF, $C_1 = 110$ nF (○) and in regime 2 for $C_0 = 266$ (●) and 376 nF (▲).

We also studied the flashlamp operation in the regimes of a freely expanding discharge and a discharge restricted by the flashlamp tube walls by exciting the lamp with a conventional *LC* generator. In the case of a freely expanding discharge, we can estimate the radiation power density at the instant corresponding to the maximum radiant intensity of the discharge.

The radius r_c' of the current channel at the instant $t_1 = 2.6(LC)^{0.5}$, corresponding to the cessation of the release of the main part of energy in the discharge, can serve as the characteristic radius of the current channel [14]. We are interested in the regimes with a high velocity of energy supply to the plasma, which provide the high brightness temperature of the plasma and the high radiation power. In such regimes, the maximum of the output radiation power is always considerably delayed with respect to the maximum of the power supplied to the discharge [14], and the estimate $t_{max} \geqslant 2.6(LC)^{0.5}$ of the time of achieving the output power maximum is valid.

At the same time, the radius of the current channel at the instant $t_2 \sim (4-5)(LC)^{0.5}$ can be estimated from the empirical expression [14]

$$r_c = 0.065(CU^2/2)^{0.4}. \quad (1)$$

This expression is also valid for discharges proceeding under various conditions and is in good agreement with our experimental data. The dependence of r_c' on the energy proves to be similar to (1) [14]. It follows from the experimental data that $r_c \approx 1.5r_c'$ [7].

As pointed out above, for discharges proceeding under various conditions, we can assume that the peak radiation power P_{max} of the flashlamp in the wavelength region 200–400 nm is proportional to the square root of the stored energy: $P_{max} \sim I_{e\,max} \sim W_0^{0.5} = (C_0U_0^2/2)^{0.5}$, irrespective of whether C_0 or U_0 is varied. This dependence is shown in Fig. 7 [curve (*1*)], where on the abscissa the energy W_0 stored in the excitation generator is plotted.

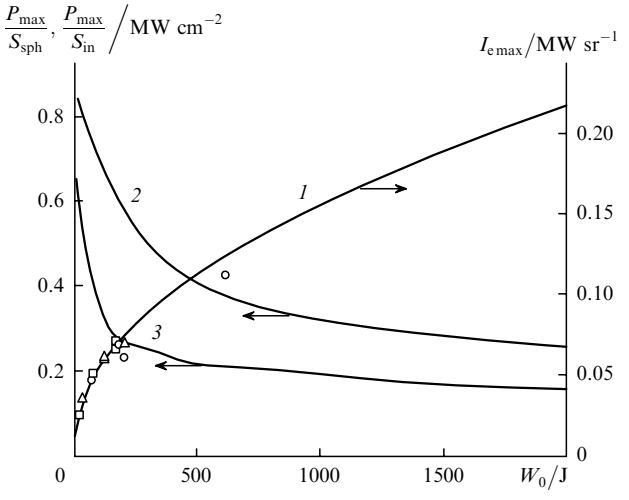

Figure 7. Dependence of the peak radiant intensity $I_{e\,max}$ of a freely expanding discharge on the energy W_0 stored in the generator (*1*) and the estimate of the radiation power density of a freely expanding discharge P_{max}/S_{sph} on the discharge plasma surface (*2*) and P_{max}/S_{in} on the inner surface (*3*) of the flashlamp at the instant of the maximum radiation power. The wavelength range is 200–400 nm, $C_0 = 266$ nF (△), 376 nF (□), and 1367 nF (○).

The maximum power density in the wavelength range 200–400 nm obtained in the experiment was, according to our estimates, ~ 110 and ~ 80 kW cm^{-2} on the internal and external surfaces of the flashlamp tube, respectively, while the radiant intensity was ~ 110 kW sr^{-1} for the stored energy of 615 J. The power density was estimated as P_{max}/S_1, where S_1 is the area of a sphere of diameter equal to the inner or outer diameter of the flashlamp tube (note that at the instant of the maximum radiation power, the discharge plasma had a shape close to spherical).

Let us estimate the radiation power density in the wavelength range 200–400 nm on the surface of the current channel for different stored energies at the instant of the maximum power. Because the empirical dependence (1) of the channel radius on the stored energy is known and $r_c' = r_c/1.5$, the power density can be estimated from the ratio P_{max}/S_{sph}, where $S_{sph} = 4\pi r_c'^2 = 4\pi(r_c/1.5)^2$ is the area of a sphere of radius r_c'. Such an estimate is valid because the real area of the plasma surface at the instant of the maximum power is $S_{pl} > S_{sph}$, and, therefore, $P_{max}/S_{pl} \leqslant P_{max}/S_{sph}$. The results of the estimate are presented in Fig. 7 [curve (*2*)]. The ordinate of the point corresponding to the energy 16 J was calculated by replacing the sphere area S_{sph} by the cylinder area $S_{cyl} = 2\pi l r_c' + 2\pi r_c'^2$, where l is the interelectrode gap, because at the instant of the maximum output radiation power the discharge plasma had a nearly cylindrical shape (as was demonstrated by the CCD photographs of the discharge [7]).

It is obvious that the power density on the surface of the plasma of a freely expanding discharge (for the maximum radiation power) lies below the obtained curve and decreases with increasing the energy stored in the generator. At the same time, the maximum radiation power density on the plasma surface and the maximum brightness of the discharge are achieved earlier than the maximum radiant intensity of the discharge (Fig. 8). Here, we estimate the radiation power density on the plasma surface from the ratio P_{uv}/S_{pl}, where P_{uv} is the UV radiation power of the discharge and the area S_{pl} of the discharge plasma surface is calculated from CCD photographs of the discharge. The diameter of the current channel at the instant of the

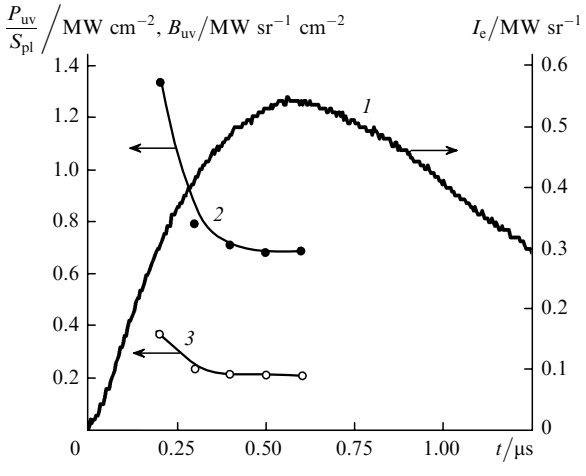

Figure 8. Time dependences of the radiant intensity I_e (*1*), the UV power density P_{uv}/S_{pl} on the plasma surface (*2*) and the brightness B_{uv} of a freely expanding discharge (*3*). The wavelength range is 200–400 nm, $C_0 = 233$ nF, $U_0 = 20$ kV.

maximum brightness was ~ 1.3 mm. The estimates of the radiation power density and brightness become valid within 200 ns after the discharge ignition (the Xe discharge photographs obtained with a CCD camera showed that a multichannel breakdown of the discharge gap almost always occurred; then, individual channels expanded and merged into one already after ~ 200 ns [7]). The maximum UV radiation power density on the discharge plasma surface was ~ 1.3 MW cm^{-2} and the maximum UV brightness of the discharge was ~ 0.37 MW sr^{-1} cm^{-2}.

When the current channel achieved the critical diameter d_{cr}, the flashlamp tube walls began to affect the channel expansion. This diameter is related to the inner diameter d_{in} of the tube by the expression $d_{cr} = 0.7 d_{in}^{1.15}$ [15]. By replacing d_{cr} with the quantity $2r_c' \leqslant d_{cr}$, we can estimate the radiation power density on the inner surface of the tube for a freely expanding discharge from the ratio P_{max}/S_{in}, where S_{in} is the area of a sphere of diameter d_{in}. The results of this estimate are presented in Fig. 7 [curve (*3*)].

By using a discharge with a steep leading edge of the radiation pulse restricted by the flashlamp walls [16], we can obtain higher power densities on the inner (and outer) surfaces of the lamp tube. Figure 9 shows the estimates of the maximum radiation power density on the inner surface of the lamp (in the wavelength range 200–400 nm). The power density was estimated from the ratio P_1/S_2, where P_1 is the discharge power density at the instant of the maximum of the power density and S_2 is the surface area of a cylinder of height equal to that of a plasma column of the discharge at the same instant and diameter equal to the outer diameter of the flashlamp tube. The duration of the radiation pulse front was shorter than 1 μs. The dependence of the power density on the stored energy has a maximum (Fig. 9). The decrease in the power density after the achievement of the maximum is caused by the reversible opaqueness of quartz walls of the flashlamp [17] (Fig. 10). The maximum UV power density on the inner and outer surfaces of the flashlamp was ~ 700 and ~ 380 kW cm^{-2}, respectively.

It is obvious that to produce a high conduction in a diamond switch, it is necessary to provide the maximum UV power density on the switch.

In the freely expanding discharge regime, the output power increases with increasing stored energy, while the power density on the lamp surfaces decreases (Fig. 7) because the minimal possible diameter of the flashlamp tube also increases with increasing energy. Therefore, to provide the efficient use of radiation from the flashlamp operating in this regime, it is necessary to employ an optical system focusing radiation on the switch and to obtain the required power density by increasing the energy stored in the excitation generator.

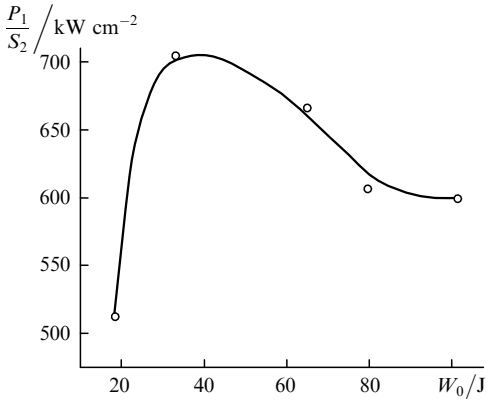

Figure 9. Dependence of the maximum radiation power density of the discharge on the inner surface of the flashlamp on the energy stored in the generator. The wavelength range is 200–400 nm, the inner diameter of the flashlamp is 3 mm, $C_0 = 165$ nF.

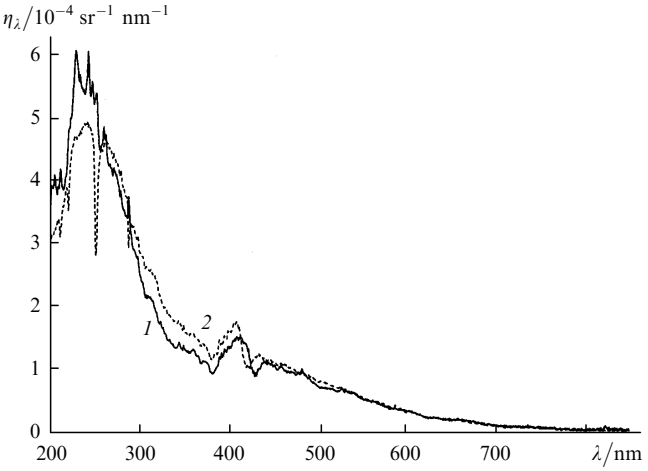

Figure 10. Spectral efficiency η_λ of the Xe flashlamp for the energy stored in the generator $W_0 = 33$ (*1*) and 101 J (*2*). The inner diameter of the flashlamp is 3 mm, $C_0 = 165$ nF.

A discharge with a steep leading edge of the radiation pulse can be obtained by placing the switch close to the quartz flashlamp tube. In addition, the flashlamp with such a discharge can be used for other applications, for example, to pump organic dye lasers.

4. Conclusions

We have studied the spectral, energy, and time characteristics of a pulsed Xe discharge by using three regimes of energy supply to the discharge and compared these regimes. It is shown that in passing from the oscillating discharge to the unidirectional current pulse regime, the output power of the radiation source increases, while the FWHM of the radiation pulse decreases.

We have compared the regimes of a freely expanding discharge and a discharge restricted by the flashlamp walls. It is shown that to produce a high conduction in the diamond switch in the freely expanding discharge regime, it is necessary to use an optical focusing system. The maximum UV power density of the plasma surface in a freely expanding discharge was ~ 1.3 MW cm^{-2} and the maximum UV brightness of the discharge was ~ 0.37 MW sr^{-1} cm^{-2}. For a discharge with a steep leading edge of the radiation pulse (shorter than 1 μs) restricted with the flashlamp walls, the maximum UV power density on the inner ad outer surfaces of the flashlamp was ~ 700 and ~ 380 kW cm^{-2}, respectively.

Acknowledgements. This work was supported by the CRDF (Grant No. RP2-538-TO-02).

References

1. Bharadwaj P.K., Code R.F., van Driel H.M., Walentynowicz E. *Appl. Phys. Lett.*, **43** (2), 207 (1983).
2. Ho P.-T., Lee C.H., Stephenson J.C., Cavanagh R.R. *Opt. Commun.*, **46**, 202 (1983).
3. Glinski J., Gu X.-J., Code R.F., van Driel H.M. *Appl. Phys. Lett.*, **45** (3), 260 (1984).
4. Krishnan M., Xu X., Schein J., Qi N., Prasad R., Gensler S. Proc. *XII IEEE Pulsed Power Conf.* (Monterey, CA, USA, 1999) p. 1222.
5. Lipatov E.I., Panchenko A.N., Tarasenko V.F., Shein J., Krishnan M. *Kvantovaya Elektron.*, 31, 1115 (2001) [*Quantum Electron.*, 31, 1115 (2001)].
6. Lomaev M.I., Rybka D.V., Tarasenko V.F., Lipatov E.I., Krishnan M., Thompson J., Rarx D. *Izv. Vysshh. Uchebn. Zaved., Ser. Fiz.*, **47**, 81 (2004).
7. Rybka D.V., Baksht E.Kh., Lomaev M.I., Tarasenko V.F., Krishnan M., Thompson J. *Zh. Tekh. Fiz.*, **75**, 131 (2005).
8. Field J.E. T*he Properties of Diamond* (London: Acad. Press, 1979).
9. Bokii G.B., Bezrukov G.N., Klyuev Yu.A., Naletov A.M., Nepsha V.I. *Prirodnye i sinteticheskie almazy* (Natural and Synthetic Diamonds) (Moscow: Nauka, 1986).
10. Fortov V.E. (Ed.) *Entsiklopediya nizkotemperaturnoi plazmy. Vvodnyi tom IV* (Encyclopaedia of Low-temperature Plasma. Introductory Vol. IV) (Moscow: Nauka, 2000).
11. Rokhlin G.N. *Razrydnye istochniki toka* (Discharge Current Sources) (Moscow: Energoatomizdat, 1991).
12. Baksht E.Kh., Panchenko A.N., Tarasenko V.F. *Kvantovaya Elektron.*, **30**, 506 (2000) [*Quantum Electron.*, 30, 506 (2000)].
13. Rukin S.N. *Prib. Tekh. Eksp.*, (4), 5 (1999).
14. Marshak I.S. (Ed.) *Impul'snye istochniki sveta* (Pulsed Light Sources) (Moscow: Energiya, 1978).
15. Dishington R.H., Hook W.R., Hilberg R.P. *App. Opt.*, **13** (10), 2300 (1974).
16. Protasov Yu.S. (Ed.) *Radiatsionnaya plazmodinamika. Tom 1* (Radiation Plasma Dynamics, Vol. 1) (Moscow: Energoatomizdat, 1991).
17. Basov Yu.G. *Istochniki nakachki mikrosekundnykh lazerov* (Pump Sources for Microsecond Lasers) (Moscow: Energoatomizdat, 1990).